Zinc-finger Nucleases as a Novel Therapeutic Strategy for Targeting Hepatitis B Virus DNAs

Thomas J Cradick[1], Kathy Keck[1], Shannon Bradshaw[2], Andrew C Jamieson[3] and Anton P McCaffrey[1]

[1]Department of Internal Medicine, University of Iowa, Iowa City, Iowa, USA; [2]Department of Mathematics and Computer Science, Drew University, Madison, New Jersey, USA; [3]Llenroc Research, Cambridge, Massachusetts, USA

Hepatitis B virus (HBV) chronically infects 350–400 million people worldwide and causes >1 million deaths yearly. Current therapies prevent new viral genome formation, but do not target pre-existing viral genomic DNA, thus curing only ~1/2 of patients. We targeted HBV DNA for cleavage using zinc-finger nucleases (ZFNs), which cleave as dimers. Co-transfection of our ZFN pair with a target plasmid containing the HBV genome resulted in specific cleavage. After 3 days in culture, 26% of the target remained linear, whereas ~10% was cleaved and misjoined tail-to-tail. Notably, ZFN treatment decreased levels of the hepatitis C virus pregenomic RNA by 29%. A portion of cleaved plasmids are repaired in cells, often with deletions and insertions. To track misrepair, we introduced an *Xba*I restriction site in the spacer between the ZFN sites. Targeted cleavage and misrepair destroys the *Xba*I site. After 3 days in culture, ~6% of plasmids were *Xba*I-resistant. Thirteen of 16 clones sequenced contained frameshift mutations that would lead to truncations of the viral core protein. These results demonstrate, for the first time, the possibility of targeting episomal viral DNA genomes using ZFNs.

Received 2 July 2009; accepted 15 January 2010; published online 16 February 2010. doi:10.1038/mt.2010.20

INTRODUCTION

Despite an effective hepatitis B virus (HBV) vaccine, ~5% of the world remains chronically infected. If untreated, 15–40% of patients will develop cirrhosis and/or hepatocellular carcinoma.[1] HBV is the ninth leading cause of death worldwide.[2] HBV is a hepadnavirus with a partially double-stranded circular DNA. Upon infection of hepatocytes, viral DNA is transported to the nucleus, where it is converted to a covalently closed, circular, double-stranded DNA (cccDNA), which remains episomal. The cccDNA is the template for transcription of the pregenomic RNA and the three main subgenomic RNAs,[3] which are translated to produce the four viral proteins (**Figure 1a**). These overlapping RNAs share a common polyadenylation site. The pregenomic RNA is reverse transcribed by the viral polymerase into the negative-strand DNA, which is converted into partially double-stranded DNA. In this regard, HBV is similar to retroviruses. Some of the partially double-stranded DNA is packaged, and some goes to the nucleus where it is filled in to become cccDNA. The estimated 15–50 copies/cell of cccDNA in the nucleus serve as a store of viral escape variants generated by the error-prone viral polymerase, which can cause drug resistance or viral rebound upon cessation of treatments.[4] Current treatments, including nucleoside analogues, block the production of viral RNA and new viral DNA, but do not attack pre-existing viral cccDNA. This may be part of the reason that current therapeutics are only effective in ~50% of patients treated.[5] The cccDNA persists in patients who were thought to have cleared the virus and in some patients diagnosed with hepatocellular carcinoma, not known to have been infected. These results strengthen the link between HBV infection and hepatocellular carcinoma, and increase our awareness of the importance of cccDNA persistence. Here, we present a possible alternative therapeutic approach that targets HBV cccDNA within cells using zinc-finger nucleases (ZFNs).

ZFNs are composed of the sequence-independent cleavage domain of the type IIs restriction enzyme *Fok*I, fused to tandem zinc-finger protein (ZFP) domains.[6] Modifying the ZFP domains can target ZFNs to novel DNA sequences.[7,8] ZFNs are very specific because two ZFP domains must bind the DNA in opposite orientation with correct spacing to permit dimerization of the *Fok*I domains and subsequent cutting of the intervening DNA (**Figure 1b**).[9–12] ZFNs containing three or four zinc-fingers are commonly used. Here, we utilize three-finger ZFNs. The α-helix of each C_2H_2 zinc-finger primarily interacts with three nucleotides in the DNA major groove.[13,14] Early *in vitro* selection experiments using randomized ZFPs, or randomized binding sites, helped establish the roles that residues at positions −1 through 6 of zinc-finger α-helices play in determining DNA-binding specificity. The target specificities of many DNA-binding helices have been published.[15–21] Amino acids at these positions can be altered to create ZFNs with novel DNA-binding specificities that have been previously published. However, modular assembly of ZFPs is hindered by the fact that zinc-finger position and context affect binding affinity and specificity.[22] We searched the HBV genome for ZFN target sites, which are generally G-rich, and rationally designed helices based on results from these studies. We then constructed a series of HBV ZFNs.

Here, we show that our rationally designed ZFNs bound and specifically cleaved an HBV sequence in cultured cells. ZFPs

Correspondence: *Anton P McCaffrey, Department of Internal Medicine, University of Iowa, MERF 3166, Iowa City, Iowa 52242, USA. E-mail: antonmccaffrey@gmail.com*

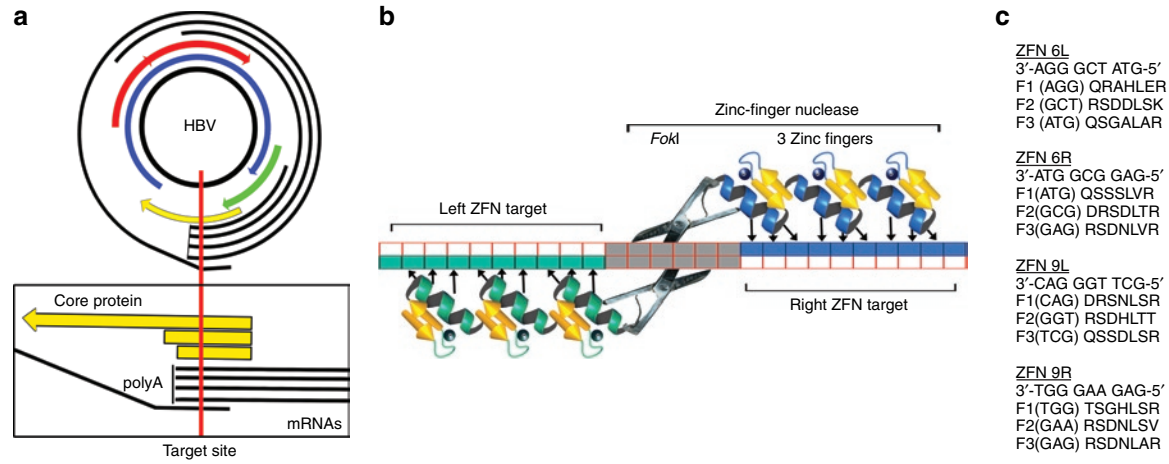

Figure 1 Zinc-finger nucleases specific for hepatitis target site. (**a**) HBV genomic DNA. The 3.2 kilobase circular HBV genomic DNA is shown with arrows representing overlapping open-reading frames. The four overlapping mRNAs are shown around the outside. The vertical line in the close-up, below, maps the ZFN 6L/6R target site's location within the core protein gene and its intersection with every HBV mRNA upstream of their common polyA sequence. The box representing the core protein open-reading frame is drawn above the shorter boxes indicating the size of the truncated proteins resulting from +1 and +2 frameshifts, which would result from among others, +4 base-pair (bp) insertions and a –7 bp deletion, respectively, as seen in the sequencing results (**Figure 6**). (**b**) Schematic of a pair of three-finger ZFNs bound to a target DNA. Arrows depict the nucleotides primarily specified by the amino acids of the binding helices. (**c**) ZFN DNA-binding helices. ZFNs bind to DNA in an antiparallel fashion. For clarity, we have listed the DNA target sequence for each ZFN 3′-5′, as opposed to the conventional orientation. Below are listed the single letter amino acid sequence codes (N to C) of positions –1 to 6 of the α-helices for each finger. F1, F2, and F3 indicate fingers 1, 2, and 3, respectively. HBV, hepatitis B virus; ZFN, zinc-finger nuclease.

without attached nucleases have been used to transiently decrease viral transcription in herpes simplex virus[23] and HBV,[24] but to our knowledge, our pair of ZFNs are the first class of therapeutics intended to directly target and inactivate episomal DNA viral genomes.

RESULTS

Design and *in vitro* testing

We searched the 3.2 kb HBV genome to identify possible binding sites for pairs of three-finger ZFNs that were separated by six nucleotides and located on opposite strands of the DNA. Each target was BLAST-searched to verify a lack of similar sequences in the human genome. Nine rationally designed ZFN pairs were assembled by overlapping PCR and cloned into a vector upstream of a *Fok*I cleavage domain (**Supplementary Figure S1a**, Materials and Methods, and data not shown). The *Fok*I domain was modified to replace 11 rare codons with common mammalian codons in order to maximize ZFN translation. The vector included cytomegalovirus (CMV) and T7 promoters (pCMV-TnT; Promega, Madison, WI) for *in vitro* and cell culture expression, respectively. ZFPs fused to the codon-optimized version of *Fok*I expressed well using coupled transcription–translation (TnT) reactions with T7 polymerase (Promega) as visualized by ^{35}S incorporation (data not shown).

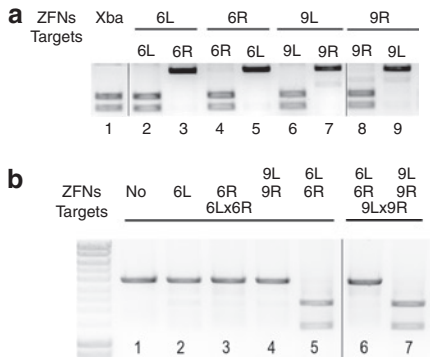

Figure 2 ZFNs specifically cleave homodimeric and heterodimeric targets in an *in vitro* cleavage assay. (**a**) *In vitro* cleavage of homodimeric targets containing two copies of the same sequence in opposite orientation. Lane 1 is an *Xba*I-digested size marker for cleaved products. Binding site plasmids are listed above each lane. Even numbered lanes are combinations of cognate ZFN and binding site plasmid, which should be cleaved. Lanes 3, 5, 7, and 9 are combinations of noncognate pairs that act as specificity controls and should not be cleaved. (**b**) *In vitro* cleavage of heterodimeric targets containing two different inverted ZFN-binding sites as they appear in the hepatitis B virus genome. A single ZFN or pairs of ZFNs are indicated at the top and binding sites are indicated below. Lanes 5 and 7 contain cognate ZFN-binding site pairs that are expected to cleave. The remaining lanes are specificity controls. ZFN, zinc-finger nuclease.

ZFN *in vitro* cleavage assays

We screened the pairs of HBV-directed ZFNs *in vitro*. Binding sites contained in the HBV genome were cloned into a 3 kb version of the plasmid, pCR4 (Invitrogen, Carlsbad, CA). The ZFNs were expressed in TnT reactions and tested using an improved version of the *in vitro* cleavage assay first described by the Chandrasegaran group[6] (Materials and Methods). For clarity, binding site plasmids were first linearized with *Xmn*I such that ZFN cleavage resulted in two bands.

We began our search for functional ZFN pairs by individually testing each ZFN's ability to cleave its homodimeric target *in vitro* (**Figure 2a**). These homodimeric targets contained two inverted copies of the same binding site, separated by a six nucleotide *Xba*I site. Previous experiments have shown that the rates

of ZFN cleavage were independent of the intervening spacer sequences, although they were dependent on spacer length (data not shown). Eight of the 18 ZFNs were able to robustly cleave their homodimeric targets *in vitro* (data not shown); six of these comprised adjacent ZFN-binding sites in the HBV genome. Based on *in vitro* cleavage efficiency, ZFN pair 6 (6L and 6R) was chosen for further testing in proof-of-principle experiments. ZFN pair 6 cuts upstream of the common polyadenylation site of the four overlapping viral mRNAs near the N-terminus of the core protein (**Figure 1a**). Cleavage at this target site therefore disrupts every viral RNA and cuts in the region that encodes the core protein, which is essential for viral packaging. Another HBV-specific ZFN pair, 9L and 9R, was used with 6L and 6R as controls, as shown in **Figures 2a,b, 3a,b, 4b, 5a**, and **7**. Binding helices for 6L, 6R, 9L, and 9R are shown in **Figure 1c**. Each ZFN demonstrated substrate specificity in the *in vitro* cleavage assay by cleaving its cognate homodimeric-binding site, but not the noncognate homodimeric-binding site (**Figure 2a**).

Heterodimeric targets were cloned with our pairs of ZFN sites in opposite orientation, as they occur in the HBV genome. To facilitate the assays described below, and to create a cleavage size marker, the intervening six nucleotides between HBV ZFN-binding sites were replaced by an *Xba*I recognition site. Neither ZFN 6L nor 6R alone cleaved the heterodimeric target, thus confirming the requirement for binding by both ZFNs in order for cleavage to occur (**Figure 2b**, lanes 2 and 3). As a pair, ZFNs 6L and 6R cleaved their heterodimeric target, but not a noncognate control target (**Figure 2b**, lanes 5 and 6, respectively). The lack of observable cleavage sites in the remaining 3 kb of binding site plasmid further demonstrates the substrate specificity of our HBV ZFNs. The control ZFNs, 9L and 9R, also cleaved their own cognate heterodimeric target, but not that of the ZFN 6 pair (**Figure 2b**, lanes 4 and 7, respectively), thus demonstrating that 9L and 9R are a functional and site-specific ZFN pair. Each ZFN set was able to cleave its target plasmids to completion, with <1 µl of TnT expression mix, in under an hour. These data are therefore the first to demonstrate specific and efficient ZFN cleavage of HBV sequences *in vitro*.

Testing of ZFN pairs in a cell culture model

To assess ZFN toxicity, we utilized a previously described assay that uses GFP transgene expression as an indicator of cell viability.[25,26] As a benchmark, we compared our ZFN pair (6L and 6R) to a published ZFN pair targeting the *CFTR* gene (CF877).[21] In contrast to our ZFN that was made by rational design and modular assembly, the CFTR ZFN pair was selected by bacterial two hybrid.[21] We co-transfected HEK-293 (**Figure 3a**) or Huh7 (**Figure 3b**) cells with an enhanced green fluorescent protein (eGFP) plasmid, a ZFN target plasmid and 0.4 µg total of ZFN pairs (6L and 6R, the noncognate 6L and 9R pair, or CF877 L and CF877 R). As a control, cells were transfected with an empty vector plasmid that expresses the *Fok*I domain with no ZFP DNA-binding domain. At days 1 and 3, four wells were trypsinized, and the percentage of eGFP$^+$ cells was determined by FACS. Transfection with 6L and 6R, or 6L and 9R caused a statistically significant decrease in eGFP$^+$ cells of ~10–15% in HEK-293 cells (**Figure 3a**). More significant toxicity was observed upon transfection with the CF877

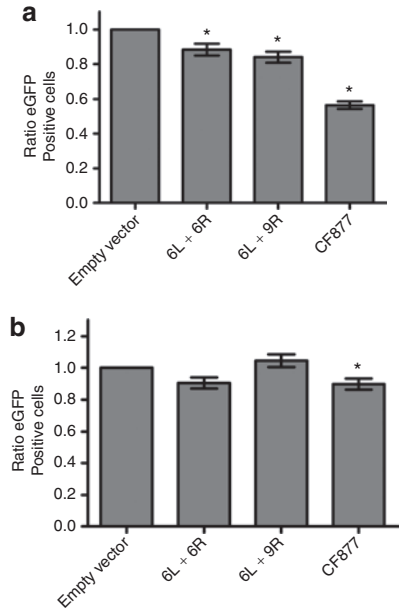

Figure 3 Assay for cellular toxicity. (**a**) HEK-293 or (**b**) Huh7 cells were co-transfected with ZFN pairs or controls, binding sites (6L and 6R, or CF877), and eGFP. Ratio of eGFP$^+$ cells at day 3/day 1 is shown. The mean of four transfections is plotted plus/minus standard error. *Statistical significance, $P < 0.05$. eGFP, enhanced green fluorescent protein; ZFN, zinc-finger nuclease.

pair (44% decrease in eGFP). No statistically significant toxicity was observed with 6L and 6R, or 6L and 9R upon transfection of Huh7 cells (**Figure 3b**). The increased toxicity observed in HEK-293 cells may be due to increased transfection efficiency in this cell type.

We next demonstrated that our HBV ZFN 6 pair was highly active in a cell culture model of HBV. Transfection of Huh7 hepatoma cells with pTHBV2 (**Supplementary Figure S1b**), an HBV genomic plasmid containing 1.3 unit lengths of HBV genome, results in full transcription of the viral RNAs, translation of the proteins and production of infectious virus.[27] We co-transfected pTHBV2 along with (i) ZFN pair 6L and 6R or (ii) 9L and 6R (which should not cleave) into Huh7 human hepatoma cells (Materials and Methods). Episomal DNA from cells transfected with pTHBV2 and 1.1 µg of ZFNs was prepared for Southern blotting using the HIRT DNA extraction protocol.[28] The DNA was digested with *Sca*I, which cuts in the plasmid backbone distant from the ZFN-binding site to create a 7.2 kb linear fragment. **Figure 4a** shows the various molecular forms that may be produced after ZFN-mediated cleavage and possible rejoining of fragments inside cells. Our oligonucleotide Southern probe only recognizes three forms, which are indicated by filled bars in **Figure 4a**. Results from three independent transfections are shown (**Figure 4b**). When cells were co-transfected with pTHBV2 plus 6L and 6R, we observed the appearance of a 4.7 kb band consistent with specific cleavage at the ZFN's target site within cells (**Figure 4b**, lanes 4–6). This band averaged 26% of the total DNA. Lanes containing DNA from cells receiving control plasmids without ZFNs did not contain bands consistent with DNA cleavage (lanes 1–3). Similarly, cleavage products were also absent in

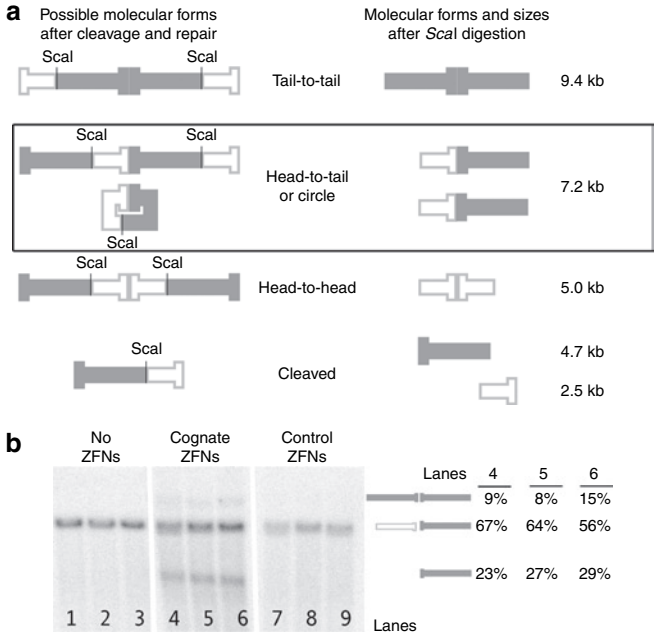

Figure 4 HBV genomic sequence is cleaved and misrepaired by ZFNs in cultured cells. (**a**) Possible molecular forms produced after ZFN-mediated cleavage and rejoining of fragments inside cultured cells. pTHBV2 could remain uncut, could be cut and recircularized (perfectly or imperfectly), could remain linear or could form concatemers (head-to-head, head-to-tail, or tail-to-tail). The various forms possible in cells are shown on the left with unique *Sca*I sites marked. For clarity, prior to Southern blotting, total DNA was *Sca*I-digested. The resulting molecular forms are indicated in the middle. Expected sizes in kilobase (kb) after *Sca*I digestion are shown to the right. The Southern blot does not allow us to distinguish between uncut, recircularized, or head-to-tail concatemerized DNAs, which all migrate at 7.2 kb. Because the oligonucleotide Southern blot probe only recognizes the sections depicted as solid (closed), it does not detect the 2.5 kb cleavage fragment or the 5 kb head-to-head concatemer. (**b**) Southern blot of ZFN-cleaved HBV DNA targets in culture cells. Huh7 cells were co-transfected with pTHBV2 and either (i) no ZFN (lanes 1–3, pCMV-LacZ stuffer), (ii) ZFN 6L and 6R (lanes 4–6) or (iii) 6L and 9R (lanes 7–9). *Sca*I-digested HIRT DNA was detected by Southern blot. Molecular forms detected are depicted in the middle, and the amounts detected of the 9.7 kb tail-to-tail concatemer, the 7.2 kb band, and the 4.7 kb linearized band in lanes 4–6 are indicated to the right. HBV, hepatitis B virus; ZFN, zinc-finger nuclease.

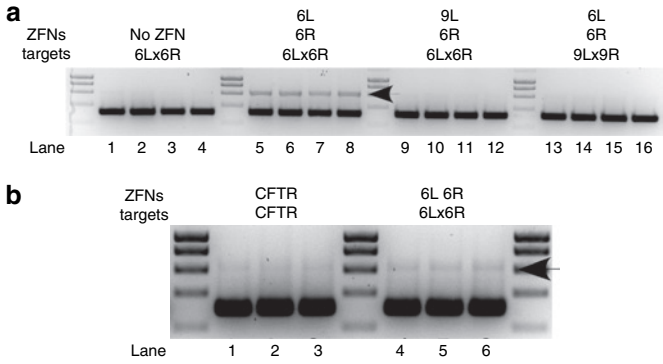

Figure 5 Nuclease resistance assay shows specific cleavage and misrepair. (**a**) Cells were transfected with the indicated target plasmid and either (i) pCMV-Fok+ with no ZFP (no ZFN, lanes 1–4), (ii) 6L and 6R (lanes 5–8), (iii) 9L and 6R (lanes 9–12) or (iv) 6L and 6R (lanes 13–16). An average of 6.2% *Xba*I-resistant fragments (lanes 5–8, upper band indicated with an arrow head, demonstrates intracellular ZFN cleavage and misrepair) were detected when 6L and 6R were co-transfected with their cognate binding site. The extent of *Xba*I digestion was greater than 99% in control lanes 1–4 and 9–16. No significant *Xba*I-resistant fragments were detected in the absence of ZFN (lanes 1–4), with control ZFN 9L and 6R (lanes 9–12) or when 6L and 6R were co-transfected with 9L and 9R, their noncognate binding sites (lanes 13–16). A molecular weight marker divides each group of four biological replicates. (**b**) Cells were transfected with cognate target plasmid and either (i) ZFN pair CF 877 (lanes 1–3) or (ii) 6L and 6R (lanes 4–6). An average of 2.1% *Xba*I-resistant fragments were seen with ZFN pair CF877, and 5.7% *Xba*I-resistant fragments were seen with ZFN pair 6L and 6R. ZFN, zinc-finger nuclease.

lanes containing DNA from cells that were transfected with ZFN 6R and a control ZFN, 9L (lanes 7–9).

Linearized free DNA ends in cells can be repaired without a template, presumably by nonhomologous end joining. Again, only in the presence of the cognate 6L and 6R ZFN pair did we observe the appearance of a 9.4 kb band corresponding to cleaved target plasmids being rejoined tail end-to-tail end (**Figure 4b**, lanes 4–6). This band averaged about 10% of the total target DNA (**Figure 4b**, lanes 4–6). Viral gene expression cannot occur when cleaved targets remain linear or when cleaved targets are incorrectly end-joined. There may be similar levels of cleaved fragments joined head-to-head, but they are not detected by this Southern probe. The Southern blot assay also did not allow determination of the amount of target cleaved and rejoined, either precisely or imprecisely, in the correct head-to-tail orientation. Importantly, the presence of the linear band demonstrates successful ZFP-mediated cleavage, and the tail-to-tail joined fragments demonstrate successful ZFP-mediated cleavage and misrepair of HBV sequences within cultured cells.

Quantitative analysis of cleavage and misrepair

The predominant 7.2 kb band in the Southern blot could represent DNA that was (i) never cleaved by a ZFN, (ii) cleaved and perfectly repaired, (iii) cleaved and imperfectly recircularized, or (iv) comprised of cleaved fragments that were joins of upstream and downstream ends of different cleaved fragments (**Figure 4a**). These possibilities cannot be distinguished by Southern blotting; therefore, we designed an assay to assess imperfect repair and concatemerization of cleaved DNA fragments (**Supplementary Figure S2**, nuclease resistance assay, Materials and Methods). In order to measure the degree of misrepair, we mutated the six nucleotide spacer sequence between the 6L and 6R binding sites to create an *Xba*I site, as we had previously done when screening ZFNs for *in vitro* activity. These target site fragments were cloned into pCR4, as in the *in vitro* cleavage assays. We reasoned that most ZFN-directed cleavage and imperfect repair would destroy the *Xba*I recognition site. We transfected cultured cells with pairs of plasmids expressing ZFNs and cognate or control heterodimeric target plasmids. After 3 days in culture, the DNA from cells treated with 0.4 µg of ZFN was HIRT-extracted and subjected to a nuclease resistance assay and sequencing.

We amplified a 610 base-pair (bp) fragment containing the HBV ZFN target region from the HIRT-extracted DNA by PCR

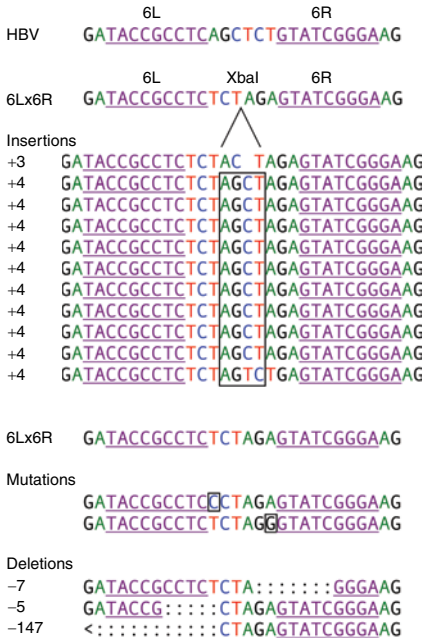

Figure 6 Sequence analysis of imperfectly repaired ZFN-cleaved HBV DNAs. DNAs from cells co-transfected with 6L and 6R and the 6L/6R binding site were PCR-amplified with primers flanking the ZFN-binding site and digested with *Xba*I (**Figure 5a**, lanes 5–8). The reactions were further amplified with nested primers and cloned for sequencing in order to determine the types of mutations present. The ZFN 6L and 6R binding sites are underlined in each sequence and in the target site in HBV and pTHBV2 (first line) and in the *Xba*I-containing 6L/6R target (second line). The insertions are listed next to the predominant 4 base-pair (bp) insertion, and the frameshift is boxed. A second 6L/6R target sequence is listed above the mutations (middle) and deletions (bottom). The 4 bp insertions and first two deletions would result in frameshifts and large truncations in the core protein–coding region of the genomic HBV DNA. The last large deletion would truncate the upstream precore protein and delete the start codon for the core protein. HBV, hepatitis B virus; ZFN, zinc-finger nuclease.

using a high fidelity polymerase (AccuPrime Pfx; Invitrogen). The PCR products were purified, *Xba*I-digested overnight and separated by agarose gel electrophoresis. The extent of *Xba*I cleavage was >99% in the absence of ZFNs (**Figure 5a**, lanes 1–4) and in control reactions (**Figure 5a**, lanes 9–16). The amplified product from cells co-transfected with ZFN 6L and 6R and their cognate target plasmid was 6% *Xba*I-resistant (**Figure 5a**, lanes 5–8, upper band, indicated with an arrow). As expected, we do not see evidence for imperfect repair of the 6Lx6R binding site when the 6L ZFN was replaced with 9L (lanes 9–12), or when 6L and 6R were co-transfected with the noncognate 9Lx9R binding site (lanes 13–16).

To asses the relative activity of our ZFN pair, we compared its activity in cells to a previously published ZFN pair targeting the cystic fibrosis (CFTR) gene that was selected using bacteria two-hybrid (ZFN pair CF 877).[21] The misrepair experiment was repeated in parallel with ZFNs targeting CF 877. The amplified product from cells co-transfected with ZFNs against CFTR and their cognate target plasmid was 2% *Xba*I-resistant (**Figure 5b**, lanes 1–3), whereas the amplified product from cells co-transfected with ZFNs 6L and 6R and their cognate target plasmid was, again, 6% *Xba*I-resistant (**Figure 5b**, lanes 5–7).

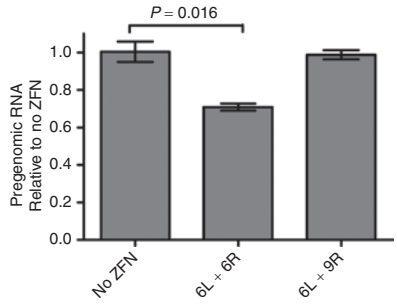

Figure 7 ZFN treatment decreases a critical viral replicative intermediate. Hepatitis B virus pregenomic RNA levels from ZFN-treated cells were measured by northern blot and normalized to GAPDH levels. Error bars represent SD. ZFN, zinc-finger nuclease.

Sequence analysis of misrepair following ZFN cleavage

We sequenced the resulting misrepaired target sequences to determine which changes had been introduced into the *Xba*I-resistant sites. This ZFN target site is largely conserved in the major strains of HBV; therefore, we believe that mutations in this region may be poorly tolerated by HBV and would thus lead to virus inactivation. The ZFN 6 target site is in the N-terminal region of the core protein–coding sequence, such that insertions and deletions there could lead to frameshifts and premature stop codons and result in large truncations of this essential viral protein. We sequenced *Xba*I-resistant target regions and aligned them with the original target sequences (**Figure 6**). Frameshift mutations were found in 13 of 16 sequences: 10 out-of-frame insertions of four bases (boxed) and three deletions. The largest deletion in our HBV target plasmid would have extended upstream and removed 104 bases of the core protein gene, including the start codon, and would have caused a truncation of the precore protein in genomic HBV. There were two sequences harboring a single mutated amino acid (boxed) and one that showed the addition of an amino acid. This range of mutations and insertions is consistent with nonhomologous end joining. These results therefore show that ZFN-mediated cleavage is often followed by repair events that interrupt viral gene expression.

Effects of ZFNs on viral fitness

We next sought to assess the effects of our ZFN treatment on viral fitness. Because cultured cells cannot be infected by HBV, we could not easily titer the yield of progeny virus. The high level of HBV plasmid transfected into the cells resulted in artifacts when quantitating viral DNA. We therefore determined the effect on replication competence by measuring the level of pregenomic RNA.[29] This RNA species is reverse transcribed to make viral DNA and can be size-differentiated by northern blotting. The northern blot signal was normalized to GAPDH (**Figure 7**). Pregenomic RNA levels in cells that were co-transfected with a mismatched pair of ZFNs (6L and 9R) were the same as in cells co-transfected with pUC19. Cells co-transfected with ZFN pair 6 showed a 29% drop in the levels of pregenomic RNA, thus demonstrating that ZFN-mediated inactivation of pTHBV2 resulted in significant reductions in this key replicative intermediate; this would be expected to reduce viral fitness.

DISCUSSION

Chronic HBV infection remains a major health problem and leading cause of death worldwide. Current therapeutics are toxic, expensive and lead to sustained virologic response (*i.e.,* viral clearance) in only ~50% of patients. We and others have hypothesized that this is due to the persistence of the HBV cccDNA. There are no current therapies that directly target episomal viral genomes for cleavage. It is possible that even partial inactivation of HBV cccDNA could have a significant therapeutic benefit. As with other antiviral drugs, HBV ZFNs would likely be used in combination with existing treatments such as interferon and nucleoside analogues, which block the formation of new cccDNA, but do not attach the existing cccDNA pool. Critically, cccDNA serves as an archive of escape mutants that allow the development of resistance to the nucleoside analogues. These existing treatments lead to multilog drops in viral titers. In combination with existing treatments, HBV ZFNs could serve as a complementary therapeutic that might slow the development of resistance HBV strains and increase the likelihood of sustained virological response.

We scanned the genome of HBV for adjacent pairs of possible ZFN-binding sites and picked nine pairs to target. For each target site, we rationally designed binding helices for the pair of ZFNs based on published specificity studies.[16–19,30] Undoubtedly, more potent ZFNs could be found with further testing or selections. Using an *in vitro* screening (**Figure 2a**), we identified a highly functional and sequence-specific HBV ZFN pair, which we tested further in cultured cells. Off-site cleavage was not detectable in the *in vitro* cleavage assays with these ZFNs (**Figure 2a,b**).

To test the ability of our HBV ZFNs to cleave sequences within the context of the full HBV genome, we employed an established HBV cell culture model wherein Huh7 human hepatoma cells were transfected with pTHBV2, a plasmid containing the entire HBV genome. We co-transfected Huh7 cells with pTHBV2 and ZFNs 6L and 6R and observed sequence-specific cleavage by a Southern blot assay. Additionally, these lanes contained bands consistent with misjoined fragments. After 3 days in culture, 26% of the target plasmid was cleaved and remained linear, and 10% was cleaved and rejoined tail-to-tail. Tail-to-tail concatemers cannot produce functional virus and DNA that remained linear would be inactive. Brunet *et al*. observed that chromosomal cleavage by two nucleases could induce chromosomal translocations at a low frequency in cultured cells.[31] The concatemerization we observed may occur by a similar mechanism. Transcription from linearized fragments would produce truncated mRNAs that would lack a polyA tail and would thus not be translated. In addition, transcription from the linear fragments or concatemers would not produce a full-length HBV core protein. We can estimate from **Figure 4b** that at least 36% of the DNA was in an inactive form at the time of measurement (linear plus concatemer). This conservative estimate does not include imperfectly repaired recircularized DNA (assayed in **Figure 5a**). Although linear DNA could be correctly recircularized at some unknown rate, it would once again become a substrate for the HBV ZFNs.

ZFNs have previously been used for targeted inactivation of chromosomal genes, such as those encoding DHFR and the CCR5 co-receptor.[32,33] Cleavage at these sites resulted in imperfect repair by nonhomologous end joining, which created insertions and deletions centered on the ZFN cleavage site, thus inactivating the gene. To measure the level of mutations at our target site, we developed an assay to measure imperfect repair, which showed that ~6% of the target sequences were cleaved and misrepaired. Sequencing revealed that 81% of these mutations resulted in frameshifts, which would lead to HBV core protein truncation at nearby stop codons. Consistent with Brunet *et al.*, our sequencing of imperfectly repaired DNAs detected a predominant four-base insertion, which is consistent with fill-in of the overhangs generated by *Fok*I followed by ligation.[31] A four bp insertion results in a +1 frameshift and creation of a stop codon 15 bp downstream of the insertion site, thus truncating the core protein by 138 amino acids in HBV strain *ayw*. The other possible frameshift (+2) results in a stop codon within 10 bp and truncation of the core protein by 141 amino acids. The largest deletion would delete the start codon of the HBV core protein. This sequence analysis also supported substrate specificity of our HBV ZFNs because mutations were centered on the target site and were not found throughout the sequenced area (data not shown).

These proof-of-concept experiments demonstrate, for the first time, effective cleavage of viral DNA targets by HBV-specific ZFNs within cultured cells. Additionally, cleaved fragments were misrepaired in a manner that could potentially inactivate HBV. The total amount of target that would be inactivated is the sum of the amount degraded, linearized and misrepaired. Importantly, co-transfection with the ZFN pair 6 decreased HBV pregenomic viral RNA levels by 29%. As the template for reverse transcription of the viral DNA, the HBV pregenomic RNA is a critical replicative intermediate. It is also the template for translation of the viral polymerase and core proteins. Thus, it is likely that reduction in pregenomic RNA levels would impact viral fitness at multiple levels.

We were encouraged by this high rate of cleavage and misrepair as well as the decrease in viral RNA during transient transfections of ZFNs and HBV model substrates because pathology from chronic HBV infection can take decades to cause significant disease. Efficiency of viral inactivation may be increased by continued expression or redelivery of ZFNs because the ZFNs would specifically target uncleaved or correctly repaired target sites, but not targets misrepaired with greater than single base insertions or deletions.

Improved results may be obtained with other ZFN pairs or with simultaneous use of multiple pairs. Use of multiple pairs in combination with existing treatments could also circumvent viral resistance. Efficiency may also be improved by screening for additional ZFN pairs, further rational design, modification of the linker to the *Fok*I domains,[9,11,12,34] or by using *Fok*I domains engineered to prevent off-site homodimerization.[35,36] Previous groups have identified functional ZFNs and subsequently used iterative rational approaches to improve the activity of these ZFNs.[34] The ZFNs could also be improved by performing selections in cells.[37,38] Whether optimized ZFNs, in combination with existing treatments, could enhance viral clearance has not yet been tested.

We are currently developing viral vectors to express these ZFNs *in vivo*. We and others have shown that self-complementary adeno-associated viral vectors are capable of transfecting essentially 100% of mouse hepatocytes. Adeno-associated viral vectors

could possibly be used to deliver ZFNs to the livers of humans. In all cases, therapeutic use requires dosage optimization. It may also be advantageous to transiently express the ZFNs from transfected mRNAs to limit the duration of ZFN expression and to minimize immune responses to ZFNs.

MATERIALS AND METHODS

Zinc-finger design. The 3.2 kb HBV genomic sequence (*ayw* strain[39]) was scanned for putative ZFN target sites consisting of GNN triplets (where N is any base) and other triplets successfully targeted by ZFPs. ZFNs were designed using helices with published specificity for three-to-four nucleotides (**Figure 1c**).[16–20,40–42] We chose the nine best target sites based on the strength of zinc-finger interactions with target sequences.

ZFN assembly and target cloning. ZFPs were assembled by a multistep PCR protocol extended from Zhang *et al.*,[43] based upon the backbone sequence of murine Zif268 and its human counterpart, EGR1. Briefly, oligonucleotides coding for each binding helix contained 15 bases of overlap with the oligonucleotides (IDT, Coralville, IA) coding for each of the backbone sequences. These were annealed and extended for eight cycles using PCR SuperMix (Invitrogen) to produce the individual ZFPs. Fingers one and two were combined and extended, as were fingers two and three, for each ZFN. The resulting two-finger products were then combined in another step of overlap PCR, before amplification (AccuPrime Pfx polymerase, Invitrogen) by outside primers containing *Ear*I restriction sites. Cleavage of these nonpalindromic sites allowed robust cloning of the tandem three-finger protein into the expression vector. We modified the catalytic domain of *Fok*I from the QQR ZFN[10] to remove 11 codons that would hinder mammalian expression. We modified the following nucleotides in *Fok*I, based on numbering starting from the first nucleotide in the linker sequence QLV: G6A, A330G, C352A, A495G, G495A, T504G, T505C, A507G, A537C, T 538C, A540G, T544C, A546G, C582A, A584G, T588C, and A591G. The modified domain was then cloned into pCMV-TnT (Promega) to make pCMV-Fok$^+$. A linker oligonucleotide was inserted with a pair of *Sap*I sites, allowing directional cloning of the ZFP inserts upstream of the *Fok*I catalytic domain in this vector, which contains both the CMV promoter for expression in mammalian cells and the T7 promoter for *in vitro* assays.

Target sequences were contained in annealed oligonucleotides (IDT) and cloned by *Pst*I and *Not*I overhangs into a version of pCR4 (Invitrogen) with the ccdB domain removed by *Eag*I digestion. Plasmids were constructed using standard techniques. All purifications (Qiagen, Valencia, CA), digestions (New England Biolabs, Beverly, MA) and rapid ligations (Roche, Indianapolis, IN) followed manufacturers' protocols.

In vitro *testing.* In order to quickly screen ZFNs, we modified the *in vitro* cleavage assay first described by the Chandrasegaran laboratory.[44] ZFNs were expressed in coupled transcription/translation reactions using rabbit reticulocyte lysates containing T7 polymerase (Promega). Expression reactions (0.5 µl) were added to 250 ng of previously *Xmn*I-linearized target plasmids, incubated at 37 °C for 1 hour in NEBuffer 4 (NEB, Beverly, MA) and resolved on agarose gels. Reference lanes were produced by digesting the linearized vectors with *Xba*I. Control reactions paired ZFNs with noncognate targets and targets with noncognate ZFNs.

Testing in tissue culture

Huh7/pTHBV2 HBV model system: Human hepatoma Huh7 cells were cultured in a humidified incubator at 37 °C and 5% CO_2 with DMEM supplemented with 10% fetal calf serum or 5% fetal calf serum (at media change after transfection) and 1% each of glutamine, pyruvate, nonessential amino acids, and penicillin–streptomycin (Invitrogen). Penicillin–streptomycin was omitted during platings for transfections. All transfections were carried out in six-well dishes at ~90% confluency using Lipofectamine 2000 (Invitrogen). Huh7 cells were transfected with pTHBV2, a plasmid containing 1.3 unit-length HBV genomes, which results in transcription of the four viral RNAs, translation of the four viral proteins, replication of partially double-stranded HBV genomic DNA, and secretion of virus into the culture media.

For **Figure 4b**, parallel triplicate sets of cells were independently transfected with 1.1 µg of the ZFN vector pair and at 3 days, cells were harvested and the DNA isolated by HIRT extraction.[28] The DNA was linearized with *Sca*I and separated by agarose gel electrophoresis. Separated DNA was transferred to a nylon membrane (Hybond N+; GE Healthcare, Piscataway, NJ). A ^{32}P end-labeled oligonucleotide Southern blot probe was used (5′-GATCTTGTTCCCAAGAATATGGTGACC-3′). Membranes were hybridized at 42 °C for 16 hours in Church's buffer (3× SSC, 5 mmol/l Tris-HCl pH 7.4, 0.5% SDS, 0.05% Ficol 400, 0.05% polyvinylpyrolidone, and 0.05% BSA) and washed three times for 30 minutes in 0.1× SSC/0.1% SDS at 42 °C. HBV DNA bands were quantitated using a PhosphorImager (GE Healthcare).

Toxicity assay. ZFN toxicity studies were carried out in HEK-293 or Huh7 cells in six-well dishes. For each cell type and condition, eight wells were transfected with 100 ng of pEGFP (Clontech, Mountain View, CA), 384 ng of target plasmids, and 0.2 µg each of the indicated ZFN vector pair or controls. At days 1 and 3, four wells were trypsinized, and cells were sorted for eGFP positivity using a Becton Dickinson FACScan (BD Biosciences, San Jose, CA). eGFP ratios were calculated as described by Maeder *et al.*,[21] except that values were normalized to empty *Fok*I vector rather than to pUC19 transfected cells. Average transfection efficiencies were 46 and 35% in HEK-293 and Huh7 cells, respectively.

Nuclease resistance assays. HEK-293 cells were cultured as described above and transfected with plasmids encoding ZFN pairs, and cognate or noncognate target plasmids. The pCMV-Fok$^+$ expression vector without a ZFP was the negative control in transfections without ZFNs. After 3 days, the cells were harvested and the DNA was HIRT-extracted.[28] The DNA was quantitated using a NanoDrop spectrophotometer (Thermo Scientific, Waltham, MA) and diluted for subsequent assays.

This HIRT-extracted DNA was amplified using primers flanking the ZF target sites, Targetup (5′ GCGGAAGAGCGCCCAATAC) and Targetdown (5′ GGCAGGAGCAAGGTGAGATG), resulting in a 610 bp fragment. The percentage of target plasmids that were cleaved and misrepaired was measured as the percentage of the PCR product that lost the *Xba*I site in the intervening space between ZFN-binding sites. Equal amounts (200 ng) of purified PCR products from each transfection were digested overnight with *Xba*I. The fragments were separated on ethidium bromide–stained agarose gels, photographed and quantified using ImageJ software (version 1.42q; NIH, Bethesda, MD). The percentage of nuclease-resistant DNA was calculated by subtracting the signal in the lower, cleaved band from the total signal. Parallel control reactions demonstrated that *Xba*I reactions went to completion.

Sequence analysis. Misrepaired target sequences were isolated by amplifying 1 µl of the *Xba*I-digested PCR products in the nuclease resistance assay. A high fidelity polymerase (Platinum Taq High Fidelity; Invitrogen) and nested primers [Targetup2 (AATACGCAAACCGCCTCTC) and Targetdown2 (TCGCCCAATAGCAGCCAGTC)] were used to amplify the products for cloning into the pCR4-Topo vector (Invitrogen) for sequencing using the T7 primer. The sequences were aligned to the 6L/6R target to map the mutations, insertions, and deletions. The frameshifts were mapped to determine the number of amino acids truncated.

Northern blot analysis. Pregenomic HBV was quantitated by northern blot, as previously described.[29] Huh7 cells were co-transfected as above with 0.5 µg of pTHBV2 and 0.2 µg each of pairs of plasmids encoding ZFN pair 6L and 6R, mismatched ZFNs 6L and 9R, or with pUC19. After 3 days, RNA was isolated and subjected to northern blot analysis. HBV RNA levels were normalized to GAPDH.

Statistical analysis. To test for toxicity of the treatments relative to no treatment in **Figure 3a,b**, a two-way ANOVA was conducted using a natural log (ln) transformation of the data, with condition (three treatments and untreated), days (1 and 3), and condition × day interaction, as the factors in the model. The data in the ln scale were used in the analysis to be able to test for effects in a relative scale, such that the difference between day 3 and day 1 means of the ln transformed data, after back transformation, corresponded to the ratio of the means in the original scale (*i.e.*, $e^{[\ln(\text{day 3}) - \ln(\text{day 1})]}$ = day 3/day 1). To compare the toxicity (day 3 to day 1 relative change) of each of the treated condition ratios with the untreated, a test of mean contrast based on the fitted ANOVA model was performed. The *P* values for these tests were adjusted using Bonferroni's method to account for multiple comparisons. The effect of each treatment relative to the untreated are shown in the toxicity graphs in **Figure 3a,b**. Note that the toxicity for each treatment represents a ratio of two ratios [*e.g.* (6L + 6R day 3/6L + 6R day 1)/(untreated day 3/untreated day 1)] that was calculated by back transformation of the ln mean differences. The standard error of the mean ratio was computed by the delta method using the mean and pooled standard error estimates from the fitted ANOVA model of the ln transformed data. A paired Student's *t*-test was used for **Figure 7**.

SUPPLEMENTARY MATERIAL

Figure S1. Plasmid maps.
Figure S2. Schematic of the nuclease resistance assay.

ACKNOWLEDGMENTS

We acknowledge Matt Porteus (University of Texas, Southwestern) for the gift of the *Fok*I domain as well as Paul McCray and Keith Joung for the CFTR ZFN pair. We thank members of the Zinc-finger Consortium for helpful discussions and Ramona McCaffrey for editorial assistance. This work was supported in part by US National Institutes of Health grant AI068885-01A1 (A.P.M.) and a Center for Gene Therapy grant DK54759 (A.P.M.). We thank M. Bridget Zimmerman from the University of Iowa Biostatistics Consulting Center for statistical analysis.

REFERENCES

1. Bruix, J and Llovet, JM (2003). Hepatitis B virus and hepatocellular carcinoma. *J Hepatol* **39** Suppl 1: S59–S63.
2. Perrillo, RP (1993). Interferon in the management of chronic hepatitis B. *Dig Dis Sci* **38**: 577–593.
3. Muzyczka, N and Berns, KI (2001). Fields Virology, **vol. 2**. Lippincott Williams and Wilkins: Philadelphia, PA. pp. 2327–2359.
4. Wu, TT, Coates, L, Aldrich, CE, Summers, J and Mason, WS (1990). In hepatocytes infected with duck hepatitis B virus, the template for viral RNA synthesis is amplified by an intracellular pathway. *Virology* **175**: 255–261.
5. Dienstag, JL, Schiff, ER, Wright, TL, Perrillo, RP, Hann, HW, Goodman, Z *et al.* (1999). Lamivudine as initial treatment for chronic hepatitis B in the United States. *N Engl J Med* **341**: 1256–1263.
6. Kim, YG, Cha, J and Chandrasegaran, S (1996). Hybrid restriction enzymes: zinc finger fusions to Fok I cleavage domain. *Proc Natl Acad Sci USA* **93**: 1156–1160.
7. Cathomen, T and Joung, JK (2008). Zinc-finger nucleases: the next generation emerges. *Mol Ther* **16**: 1200–1207.
8. Carroll, D (2008). Progress and prospects: zinc-finger nucleases as gene therapy agents. *Gene Ther* **15**: 1463–1468.
9. Bibikova, M, Carroll, D, Segal, DJ, Trautman, JK, Smith, J, Kim, YG *et al.* (2001). Stimulation of homologous recombination through targeted cleavage by chimeric nucleases. *Mol Cell Biol* **21**: 289–297.
10. Porteus, MH and Baltimore, D (2003). Chimeric nucleases stimulate gene targeting in human cells. *Science* **300**: 763.
11. Smith, J, Bibikova, M, Whitby, FG, Reddy, AR, Chandrasegaran, S and Carroll, D (2000). Requirements for double-strand cleavage by chimeric restriction enzymes with zinc finger DNA-recognition domains. *Nucleic Acids Res* **28**: 3361–3369.
12. Händel, EM, Alwin, S and Cathomen, T (2009). Expanding or restricting the target site repertoire of zinc-finger nucleases: the inter-domain linker as a major determinant of target site selectivity. *Mol Ther* **17**: 104–111.
13. Pavletich, NP and Pabo, CO (1991). Zinc finger-DNA recognition: crystal structure of a Zif268-DNA complex at 2.1 A. *Science* **252**: 809–817.
14. Elrod-Erickson, M, Rould, MA, Nekludova, L and Pabo, CO (1996). Zif268 protein-DNA complex refined at 1.6 A: a model system for understanding zinc finger-DNA interactions. *Structure* **4**: 1171–1180.
15. Choo, Y and Klug, A (1994). Toward a code for the interactions of zinc fingers with DNA: selection of randomized fingers displayed on phage. *Proc Natl Acad Sci USA* **91**: 11163–11167.
16. Segal, DJ, Dreier, B, Beerli, RR and Barbas, CF 3rd (1999). Toward controlling gene expression at will: selection and design of zinc finger domains recognizing each of the 5′-GNN-3′ DNA target sequences. *Proc Natl Acad Sci USA* **96**: 2758–2763.
17. Dreier, B, Beerli, RR, Segal, DJ, Flippin, JD and Barbas, CF 3rd (2001). Development of zinc finger domains for recognition of the 5′-ANN-3′ family of DNA sequences and their use in the construction of artificial transcription factors. *J Biol Chem* **276**: 29466–29478.
18. Liu, Q, Xia, Z, Zhong, X and Case, CC (2002). Validated zinc finger protein designs for all 16 GNN DNA triplet targets. *J Biol Chem* **277**: 3850–3856.
19. Dreier, B, Fuller, RP, Segal, DJ, Lund, CV, Blancafort, P, Huber, A *et al.* (2005). Development of zinc finger domains for recognition of the 5′-CNN-3′ family DNA sequences and their use in the construction of artificial transcription factors. *J Biol Chem* **280**: 35588–35597.
20. Choo, Y and Klug, A (1994). Selection of DNA binding sites for zinc fingers using rationally randomized DNA reveals coded interactions. *Proc Natl Acad Sci USA* **91**: 11168–11172.
21. Maeder, ML, Thibodeau-Beganny, S, Osiak, A, Wright, DA, Anthony, RM, Eichtinger, M *et al.* (2008). Rapid "open-source" engineering of customized zinc-finger nucleases for highly efficient gene modification. *Mol Cell* **31**: 294–301.
22. Ramirez, CL, Foley, JE, Wright, DA, Müller-Lerch, F, Rahman, SH, Cornu, TI *et al.* (2008). Unexpected failure rates for modular assembly of engineered zinc fingers. *Nat Methods* **5**: 374–375.
23. Papworth, M, Moore, M, Isalan, M, Minczuk, M, Choo, Y and Klug, A (2003). Inhibition of herpes simplex virus 1 gene expression by designer zinc-finger transcription factors. *Proc Natl Acad Sci USA* **100**: 1621–1626.
24. Zimmerman, KA, Fischer, KP, Joyce, MA and Tyrrell, DL (2008). Zinc finger proteins designed to specifically target duck hepatitis B virus covalently closed circular DNA inhibit viral transcription in tissue culture. *J Virol* **82**: 8013–8021.
25. Cornu, TI, Thibodeau-Beganny, S, Guhl, E, Alwin, S, Eichtinger, M, Joung, JK *et al.* (2008). DNA-binding specificity is a major determinant of the activity and toxicity of zinc-finger nucleases. *Mol Ther* **16**: 352–358.
26. Pruett-Miller, SM, Connelly, JP, Maeder, ML, Joung, JK and Porteus, MH (2008). Comparison of zinc finger nucleases for use in gene targeting in mammalian cells. *Mol Ther* **16**: 707–717.
27. Marion, PL, Salazar, FH, Liittschwager, K, Bordier, BB, Seeger, C, Winters, MA *et al.* (2003). *A transgenic mouse lineage useful for testing antivirals targeting hepatitis B virus.* In: Schinazi, RF, Rice, C and Sommadossi, JP (eds). Frontiers in Viral Hepatitis. Elsevier Science: Amsterdam. pp 197–209.
28. Hirt, B (1967). Selective extraction of polyoma DNA from infected mouse cell cultures. *J Mol Biol* **26**: 365–369.
29. Keck, K, Volper, EM, Spengler, RM, Long, DD, Chan, CY, Ding, Y *et al.* (2009). Rational design leads to more potent RNA interference against hepatitis B virus: factors effecting silencing efficiency. *Mol Ther* **17**: 538–547.
30. Porteus, MH (2006). Mammalian gene targeting with designed zinc finger nucleases. *Mol Ther* **13**: 438–446.
31. Brunet, E, Simsek, D, Tomishima, M, DeKelver, R, Choi, VM, Gregory, P *et al.* (2009). Chromosomal translocations induced at specified loci in human stem cells. *Proc Natl Acad Sci USA* **106**: 10620–10625.
32. Santiago, Y, Chan, E, Liu, PQ, Orlando, S, Zhang, L, Urnov, FD *et al.* (2008). Targeted gene knockout in mammalian cells by using engineered zinc-finger nucleases. *Proc Natl Acad Sci USA* **105**: 5809–5814.
33. Perez, EE, Wang, J, Miller, JC, Jouvenot, Y, Kim, KA, Liu, O *et al.* (2008). Establishment of HIV-1 resistance in CD4+ T cells by genome editing using zinc-finger nucleases. *Nat Biotechnol* **26**: 808–816.
34. Urnov, FD, Miller, JC, Lee, YL, Beausejour, CM, Rock, JM, Augustus, S *et al.* (2005). Highly efficient endogenous human gene correction using designed zinc-finger nucleases. *Nature* **435**: 646–651.
35. Szczepek, M, Brondani, V, Büchel, J, Serrano, L, Segal, DJ and Cathomen, T (2007). Structure-based redesign of the dimerization interface reduces the toxicity of zinc-finger nucleases. *Nat Biotechnol* **25**: 786–793.
36. Miller, JC, Holmes, MC, Wang, J, Guschin, DY, Lee, YL, Rupniewski, I *et al.* (2007). An improved zinc-finger nuclease architecture for highly specific genome editing. *Nat Biotechnol* **25**: 778–785.
37. Hurt, JA, Thibodeau, SA, Hirsh, AS, Pabo, CO and Joung, JK (2003). Highly specific zinc finger proteins obtained by directed domain shuffling and cell-based selection. *Proc Natl Acad Sci USA* **100**: 12271–12276.
38. Joung, JK, Ramm, EI and Pabo, CO (2000). A bacterial two-hybrid selection system for studying protein-DNA and protein-protein interactions. *Proc Natl Acad Sci USA* **97**: 7382–7387.
39. Galibert, F, Mandart, E, Fitoussi, F, Tiollais, P and Charnay, P (1979). Nucleotide sequence of the hepatitis B virus genome (subtype ayw) cloned in E. coli. *Nature* **281**: 646–650.
40. Isalan, M, Klug, A and Choo, Y (1998). Comprehensive DNA recognition through concerted interactions from adjacent zinc fingers. *Biochemistry* **37**: 12026–12033.
41. Moore, M, Klug, A and Choo, Y (2001). Improved DNA binding specificity from polyzinc finger peptides by using strings of two-finger units. *Proc Natl Acad Sci USA* **98**: 1437–1441.
42. Fu, F, Sander, JD, Maeder, M, Thibodeau-Beganny, S, Joung, JK, Dobbs, D *et al.* (2009). Zinc Finger Database (ZiFDB): a repository for information on C2H2 zinc fingers and engineered zinc-finger arrays. *Nucleic Acids Res* **37**(Database issue): D279–D283.
43. Zhang, L, Spratt, SK, Liu, Q, Johnstone, B, Qi, H, Raschke, EE *et al.* (2000). Synthetic zinc finger transcription factor action at an endogenous chromosomal site. Activation of the human erythropoietin gene. *J Biol Chem* **275**: 33850–33860.
44. Smith, J, Berg, JM and Chandrasegaran, S (1999). A detailed study of the substrate specificity of a chimeric restriction enzyme. *Nucleic Acids Res* **27**: 674–681.